NACA L-70

NATIONAL ADVISORY COMMITTEE FOR AERONAUTICS

WARTIME REPORT

ORIGINALLY ISSUED

July 1945 as
Restricted Bulletin L5F15

THEORETICAL AND EXPERIMENTAL DYNAMIC LOADS

FOR A PRISMATIC FLOAT HAVING AN

ANGLE OF DEAD RISE OF $22\frac{1}{2}^{\circ}$

By Wilbur L. Mayo

Langley Memorial Aeronautical Laboratory
Langley Field, Va.

NACA

WASHINGTON

NATIONAL ADVISORY COMMITTEE FOR AERONAUTICS

RESTRICTED BULLETIN

THEORETICAL AND EXPERIMENTAL DYNAMIC LOADS FOR A PRISMATIC FLOAT HAVING AN ANGLE OF DEAD RISE OF $22\frac{1}{2}^{\circ}$

By Wilbur L. Mayo

SUMMARY

An application of a modified hydrodynamic impact theory is presented. Plots are given from which the maximum load, the time to reach maximum load, and the variation of load with time may be obtained for a prismatic float of $22\frac{1}{2}^{\circ}$ angle of dead rise for different combinations of flight-path angle, trim, weight, velocity, and fluid density. The curves cover the range of trim, flight-path angle, and weight-velocity relationship for conventional airplanes. Test data obtained in the Langley impact basin are presented and are used to establish the validity of the theoretical curves.

INTRODUCTION

During the past 15 years numerous reports have been written on hydrodynamic theory for the landing impact of seaplane floats but none of these treatments has been accepted for design purposes. An analysis (unpublished) of available treatments (references 1 to 8) was undertaken by the Langley Laboratory in order to determine the validity and possibilities of the theory. This analysis showed that the previous treatments did not properly take into account certain hydrodynamic forces, particularly those associated with planing action.

An application of a modified hydrodynamic impact theory is presented herein for the case of a rigid prismatic float having an angle of dead rise of $22\frac{1}{2}^{\circ}$. The validity of this theory is established experimentally by

comparison with data for a rigid float tested in the Langley impact basin. The theoretical solutions are directly applicable to the calculation of the dynamic response of elastic airframes, if it is assumed that the variation of load with time is not substantially affected by the structural elasticity of the body. Experimental verification of the rigid-body equations is significant in that it establishes the validity of a basic hydrodynamic theory which is equally applicable to the derivation of equations that involve modification of the force history due to structural elasticity. Additional work is planned to include the effect of the structural response on the loading function.

A large number of force histories is given by three plots from which the maximum load, the time to reach maximum load, and the variation of load with time may be obtained. The equations used in obtaining the results are given and the method of solution is explained in an appendix.

SYMBOLS

β angle of dead rise, degrees

τ trim, degrees

γ flight-path angle, degrees

W weight of float

V resultant velocity at instant of first contact with water surface

ρ mass density of fluid

g acceleration of gravity

$t_{a_{max}}$ elapsed time between instant of first contact with water surface and instant of maximum acceleration

m mass of float

$n_{i_{w_{max}}}$ impact load factor (maximum hydrodynamic load normal to water surface divided by W)

Where units are not given, any consistent system of units may be used.

RESULTS

Comparison of Theory and Experiment

Theoretical solutions made for a rigid prismatic float having an angle of dead rise of $22\frac{1}{2}^{\circ}$ were compared with data obtained from tests of a float having the form of the forebody shown in figure 1 and the offsets given in table I. The agreement obtained in this comparison indicates that the theory can be applied to floats which do not differ from a prism more than the float in figure 1. Figure 2 shows the variation of the impact-load-factor coefficient with flight-path angle for trims ranging from 3° to 12°. The equations, from which the curves were obtained, were derived on the assumption that the ratios of fluid compressibility, viscous forces, and gravity forces to inertia forces are negligible. In tank tests of seaplanes the ratio of the gravity forces to the inertia forces (Froude's number) is the criterion for determining the similarity of the flow for similar hulls of different size. The high speed associated with an impact tends to increase the inertia forces and to decrease the relative importance of the gravity forces; however, the tendency to design large airplanes to have landing speeds of the same order as small airplanes results in lesser acceleration for the larger weights and greater importance of the gravity forces. For a specific landing speed there is a weight range above which the gravity forces may be of substantial importance.

Experimental data are included in figure 2 for the two boundary values of trim investigated. The data were obtained at widely different speeds for a float weighing 1100 pounds. Even the points obtained in low-speed tests, for which gravity forces are of greater importance than for high-speed tests, show remarkable agreement with computations made on the assumption that the gravity forces are negligible. For a full-scale landing speed of 70 miles per hour the experimental data represent airplanes weighing up to 160,000 pounds. For higher landing speeds, such as may occur with military airplanes, the represented weight is even greater. These interpretations of the experimental check show that the theoretical computations presented

herein will give good results for all present-day airplanes. Pertinent data with regard to the weight-velocity relationships for equal ratios of the gravity forces to the inertia forces $\left(\text{equivalent values of } V\left(\frac{\rho}{g^2 W}\right)^{1/6}\right)$ are included in figure 2.

The fact that the curves in figure 2 intersect shows that the variation of maximum impact force with trim for large flight-path angles is the reverse of the variation for small flight-path angles. For small flight-path angles the planing forces predominate and, since the effect of increased trim is to increase the downwash angle of the deflected stream, the resulting increase of the resultant force for a specific draft at the step causes the impact to be more severe than for small trim. For large flight-path angles the increase of the virtual mass due to vertical velocity dominates the impact force and, since the effect of increased trim is to lower the rate of increase of the virtual mass for a specific vertical velocity, lesser force for a specific draft, and consequently a less severe impact than for small trim, occurs.

Figure 3 shows the variation of the time to reach maximum acceleration with flight-path angle for trims ranging from 3° to 12°. The plot is similar to figure 2 and therefore does not require further explanation.

Figure 4 is a plot of acceleration ratio against time ratio for a wide range of flight-path angle and trim. The ratios are based on the acceleration and time at any instant as compared with the maximum acceleration and the time to reach maximum acceleration. By interpolating between the curves of figure 4 and using the amplitude and time plots of figures 2 and 3 to define the maximum acceleration and the time to reach maximum acceleration, any number of time histories within the range of investigated conditions can be constructed.

Because individual curves would be difficult to distinguish if all the solutions of the equations given in the appendix were plotted, some of the solutions have been grouped and the boundary lines for each group plotted in figure 4. The solutions that lie between the boundary lines are tabulated in figure 4. Although an approximate interpolation can be effected between the boundary lines of figure 4, the spacing is close enough to permit the use of a line centered between these boundaries for practical solutions.

The equations used to obtain figures 2 to 4 assume that the beam of the float is large enough to prevent the chine from coming into firm contact with the water. If the chine does come into contact with the water, a discontinuity occurs in the impact process and the conditions specified by the equations of this report for the time of chine contact must be taken as the initial conditions for a different equation for the case of immersed chines. It is planned that a later program will deal with such calculations.

Applicability to Flight Impact

The load values given herein are based on the assumption that the chines do not become immersed; it should be noted that early immersion of the chines can cause only reduction of the maximum load and hence conservative load values. The variation of the impact force with draft, which was obtained in the course of solving the equations of the appendix for the force-time variation, was used to determine the effects of beam loading, flight-path angle, and trim on chine immersion. A comparison of the data obtained in this study with available data for a number of different airplanes was made. It was indicated that the beam loadings of conventional American seaplanes and flying boats are sufficiently light to ensure that maximum load values given herein will not be unduly conservative. Some German airplanes, and possibly some American flying boats with wartime overload, have high beam loadings, which may cause the immersion of the chines to be significant for high trims and steep flight-path angles.

For small angles of dead rise and for large trims the theory requires a different formula. Since the exact manner of the transformation from the condition requiring one formula to the condition requiring another formula is not known, the formulas of the appendix should not be applied indiscriminately.

The equations presented are for the absence of pulled-up bow. The bow of the float tested is representative of the bow of an actual flying boat; agreement between the data obtained and the theoretical computations for the prismatic float indicates that the effect of the bow is not important for the conditions investigated.

Both the experimental data and the theoretical calculations are for fixed-trim impact and therefore do not indicate the effect of angular rotation during impact. Various design considerations tend to locate the center of gravity relative to the center of water pressure so as to minimize angular acceleration. Even when substantial angular accelerations are reached, the time to reach peak load is believed to be short enough and the average angular velocity small enough to keep large angular displacement from being reached during this period.

The experimental data used in the present report were obtained in tests of the float shown in figure 1 with the afterbody removed. Although exact evaluation of the effects of afterbody loads is not possible at this time, various design considerations ensure that actual airplanes will have sufficient depth of the step and reduced trim at the afterbody to be effective in promoting the shielding, at impact speed, of the afterbody by the forebody and in causing thereby the loads on the afterbody to be of relatively small importance.

The experimental data used herein were obtained with a float attached to a coasting carriage having a mass about three times the mass of the float. This condition involves slight reduction of the speed during impact, whereas in the theoretical computations a constant horizontal speed is assumed. By observing the relative magnitudes of the vertical and horizontal accelerations and velocities for an impact and applying the laws of velocity dissipation, even in the case in which the float is entirely free in the drag direction, the reduction in horizontal speed during the impact can be seen to be of small importance. By using different constants in the equations of the appendix, the reduction in horizontal speed can be incorporated; however, it is felt that the gain would be too slight to warrant the additional complication.

The curves of the present report are for smooth-water impacts but they will give approximate results for rough-water impacts if the flight-path angle and the trim are defined relative to the wave surface rather than relative to the horizontal.

The equations in the appendix are based on the assumption that the float is weightless (1g wing lift). Deviation of the wing lift of the actual airplane from 1g will affect the experimental results but the effect will probably not be very large.

CONCLUSIONS

Application of a modified hydrodynamic impact theory to a rigid prismatic float with angle of dead rise of $22\frac{1}{2}^{\circ}$ and an analysis of data made to determine the validity of the theory indicate the following conclusions:

1. The effect of trim on load for large flight-path angles is the reverse of that for small flight-path angles. This reversal is due to a change in the relative importance of the planing and impact forces and shows that both the forces must be considered.

2. The agreement between experiment and theory was good, and thus the theory was proved adequate for the conditions investigated.

3. Since hydrodynamic impact theory does not take into account the effect of the gravity forces on the fluid flow, the agreement of this theory with experiment for the range of weight-velocity relationships for landing impacts of present-day airplanes indicated that the effect of gravity on the flow pattern is not important in impacts of such airplanes.

4. Consideration of the factors involved in applying the theoretical curves to actual airplanes indicated that such applications will give good results.

Langley Memorial Aeronautical Laboratory
National Advisory Committee for Aeronautics
Langley Field, Va.

APPENDIX

MATHEMATICAL FORMULAS AND METHOD OF SOLUTION

The following formulas were used in computing the curves of this report:

$$y^3 = \frac{6m \sin\tau \cos^2\tau}{(A-B)C}\left\{\left[\left(\frac{\frac{\dot{y}}{\dot{y}_o}\tan\gamma + \frac{A\sin\tau\cos\tau}{A-B\sin^2\tau}}{\tan\gamma + \frac{A\sin\tau\cos\tau}{A-B\sin^2\tau}}\right)^{\frac{A\cot^2\tau}{A-B\sin^2\tau}}\left(\frac{\tan\gamma + \tan\tau}{\frac{\dot{y}}{\dot{y}_o}\tan\gamma + \tan\tau}\right)^{\csc^2\tau}\right]-1\right\} \qquad (1)$$

$$-\ddot{y} = 3Cy^2\frac{\left(\dot{y} + \dot{y}_o\frac{\tan\tau}{\tan\gamma}\right)\left[\dot{y}\left(A - B\sin^2\tau\right) + \frac{A\dot{y}_o\sin\tau\cos\tau}{\tan\gamma}\right]}{6m\sin\tau\cos^2\tau + (A-B)Cy^3} \qquad (2)$$

In equations (1) and (2)

$$A = 0.75\pi\rho\left(\frac{\pi}{2\beta} - 1\right)^2 + 0.79\frac{\rho}{\tan\beta}$$

$$B = 0.79\frac{\rho}{\tan\beta}$$

$$C = 1 - \frac{\tan\tau}{2\tan\beta}$$

where β is measured in radians and

y draft of float at any instant

$\dot{y}_o$ vertical velocity at contact

$\dot{y}$ vertical velocity of float at any instant

$\ddot{y}$ vertical acceleration of float at any instant

Formulas (1) and (2) are not applicable when y is negative, that is, after the float has rebounded from the water surface. These solutions, which can be readily obtained from equation (2), lie in the region where y is negative. Efforts to obtain a solution giving the displacement explicitly as a function of the time have not been successful and, consequently, the following procedure was used to calculate the curves presented herein:

1. Substitute arbitrary values of $\dot{y}$ in equation (1) and solve for the corresponding values of y.

2. Substitute corresponding values of $\dot{y}$ and y in equation (2) and calculate the corresponding values of $\ddot{y}$.

3. Repeat process for values of $\dot{y}$ selected to define adequately the $\ddot{y}$-curves with a minimum number of points.

4. Plot the variation of $1/\dot{y}$ with y. For each point on this curve the acceleration is known from the previous steps. The time for each combination of y, $\dot{y}$, and $\ddot{y}$ can be obtained by integrating the area beneath and to the left of a particular point on the curve showing the variation of $1/\dot{y}$ with y. Determine such time values for intervals that approximately define the acceleration-time curve. Repeat the process for such y

and $\dot{y}$ combinations as are of greatest help in defining the more critical portions of this curve.

The accuracy of the outlined method is dependent upon the number of points for which solutions are made in order to fair the various curves. After a certain amount of experience with these solutions, the accuracy of a specific solution may be approximated by estimating possible errors involved in fairing the curves through the limited number of points. It has been found that after the constants for equations (1) and (2) are computed curves giving the relations between acceleration, velocity, and draft within an accuracy of the order of 1 percent can be obtained by one computer in 3 or 4 hours.

REFERENCES

1. von Kármán, Th.: The Impact on Seaplane Floats during Landing. NACA TN No. 321, 1929.

2. Pabst, Wilhelm: Theory of the Landing Impact of Seaplanes. NACA TM No. 580, 1930.

2. Pabst, Wilhelm: Landing Impact of Seaplanes. NACA TM No. 624, 1931.

4. Wagner, Herbert: Landing of Seaplanes. NACA TM No. 622, 1931.

5. Wagner, Herbert: Über Stoss- und Gleitvorgänge an der Oberfläche von Flüssigkeiten. Z.f.a.M.M., Bd. 12, Heft 4, Aug. 1932, pp. 193-215.

6. Schmieden, C.: Über den Landestoss von Flugzeugschwimmern. Ing.-Archiv., Bd. X, Heft 1, Feb. 1939, pp. 1-13.

7. Sydow, J.: Über den Einfluss von Federung und Kielung auf den Landestoss. Jahrb. 1938 der deutschen Luftfahrtforschung, R. Oldenbourg (Munich), pp. I 329 - I 338. (Available as British Air Ministry Translation No. 861.)

8. Kreps, R. L.: Experimental Investigation of Impact in Landing on Water. NACA TM No. 1046, 1943.

TABLE I.- OFFSETS OF LANGLEY IMPACT BASIN FLOAT MODEL M-1 (SEE FIG. 1)

[All dimensions are in inches]

Station	Half-breadth		Height above datum line			Height above keel	
	Chine	Deck	Keel	Chine	Deck	Chine	Deck
0	0	0	21.99	21.99	29.01	0	7.02
2	2.01	1.45	15.45	21.80	29.58	6.35	14.13
5	4.70	3.05	11.99	23.26	30.22	11.27	18.23
9	7.60	4.58	8.95	23.19	30.92	14.24	21.97
14	10.17	5.93	6.44	21.20	31.50	14.76	25.06
21	12.81	7.23	4.16	18.35	31.93	14.19	27.77
29	15.09	8.15	2.55	15.60	32.00	13.05	29.45
38	16.36	8.71	1.44	13.14		11.70	30.56
47	18.04	8.94	.72	11.27		10.55	31.28
58	18.87	9.00	.22	9.63		9.41	31.78
72	19.33		.02	8.31		8.29	31.93
87.25	19.40		0	7.91		7.91	32.00
106.625	19.40		0	7.91		7.91	32.00
[a]120.75F	19.40		0	7.91		7.91	32.00
[b]120.75A	18.67		1.95	9.54		7.59	30.05
137	17.83		3.95	11.41		7.46	28.05
153	16.85		5.91	13.18		7.27	26.09
169	15.65	8.82	7.87	14.81		6.94	24.13
185	14.00	8.09	9.84	16.17		6.33	22.16
201	11.74	6.54	11.77	17.24		5.47	20.23
216	8.59	4.13	13.66	17.69		4.03	18.34

[a]Forebody.
[b]Afterbody.

NATIONAL ADVISORY
COMMITTEE FOR AERONAUTICS

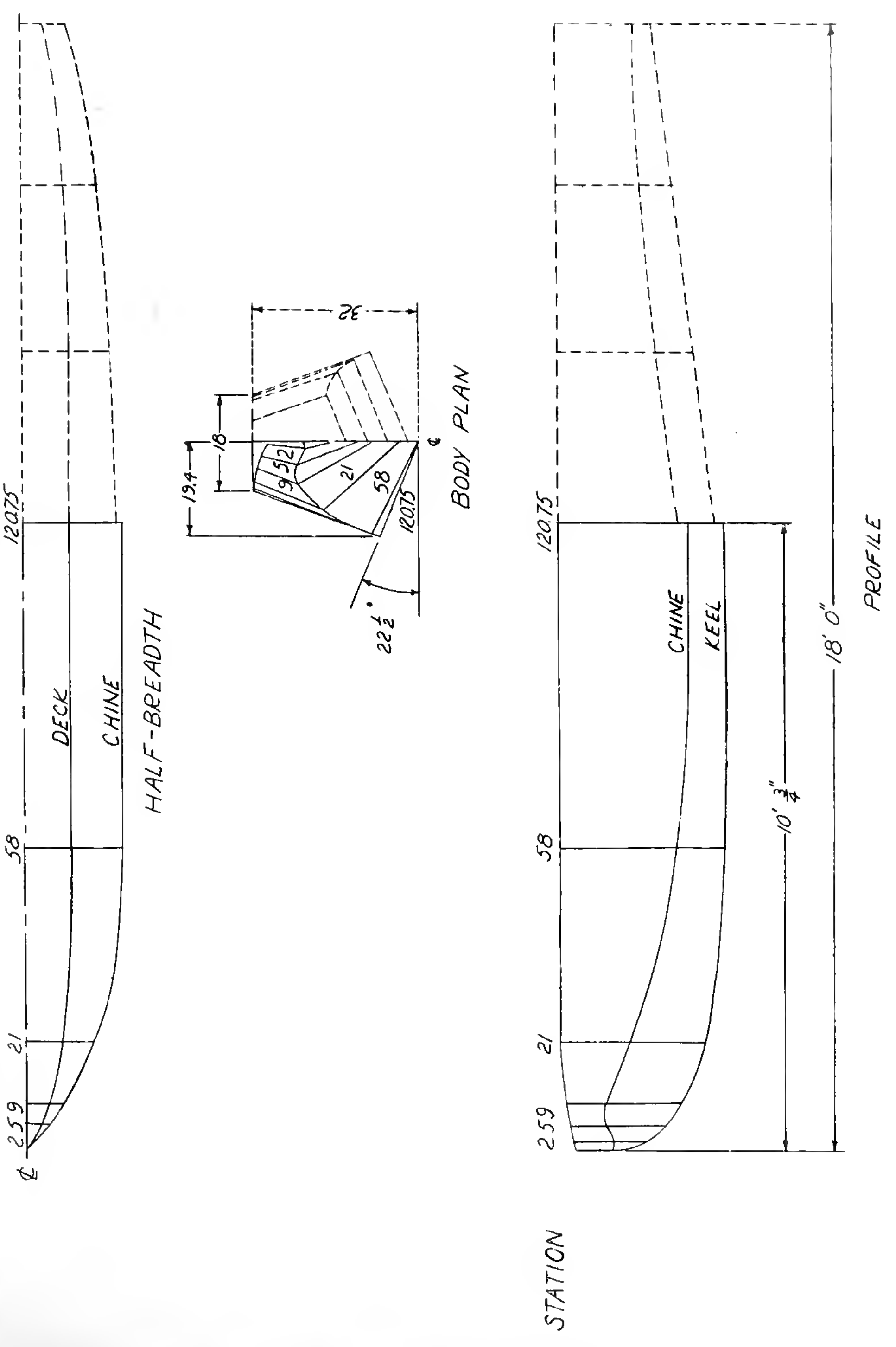

FIGURE 1.-LANGLEY IMPACT BASIN FLOAT MODEL M-1.
OFFSETS GIVEN IN TABLE I.

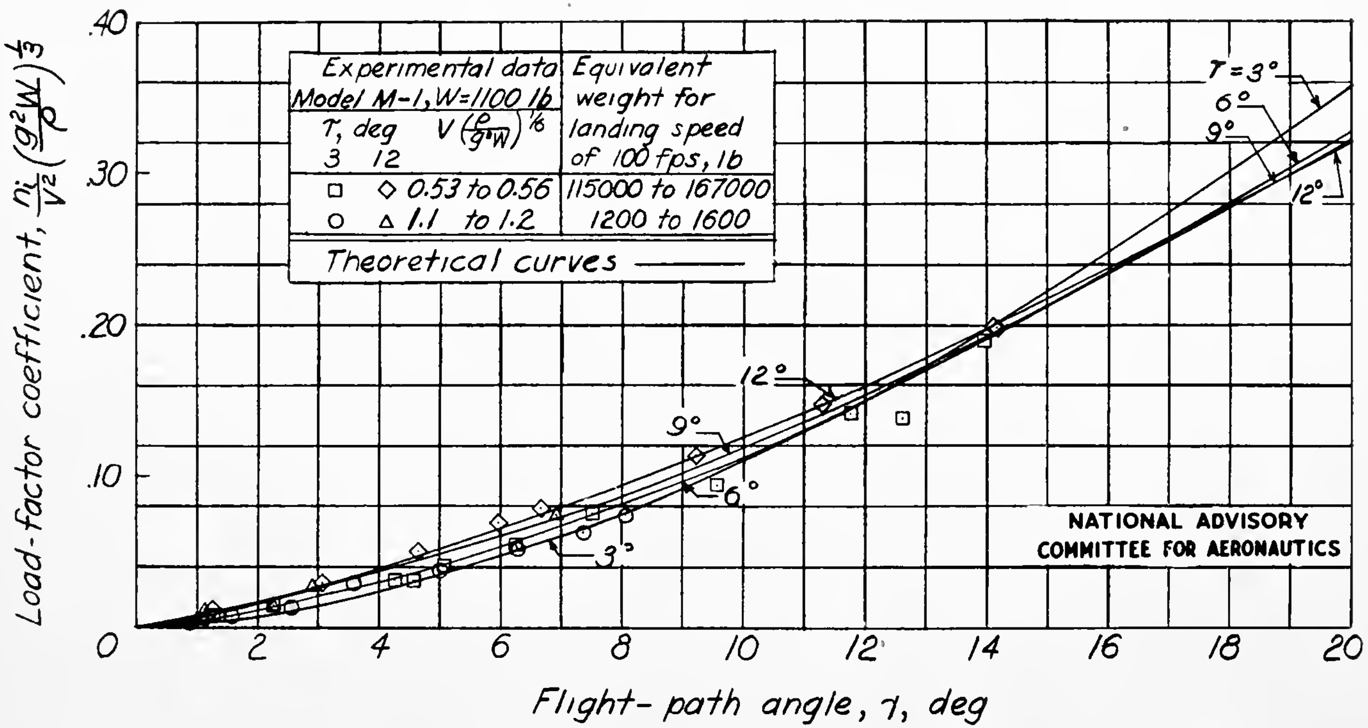

Figure 2.- Variation of load-factor coefficient with flight-path angle for a prismatic float having an angle of dead rise of $22\frac{1}{2}°$.

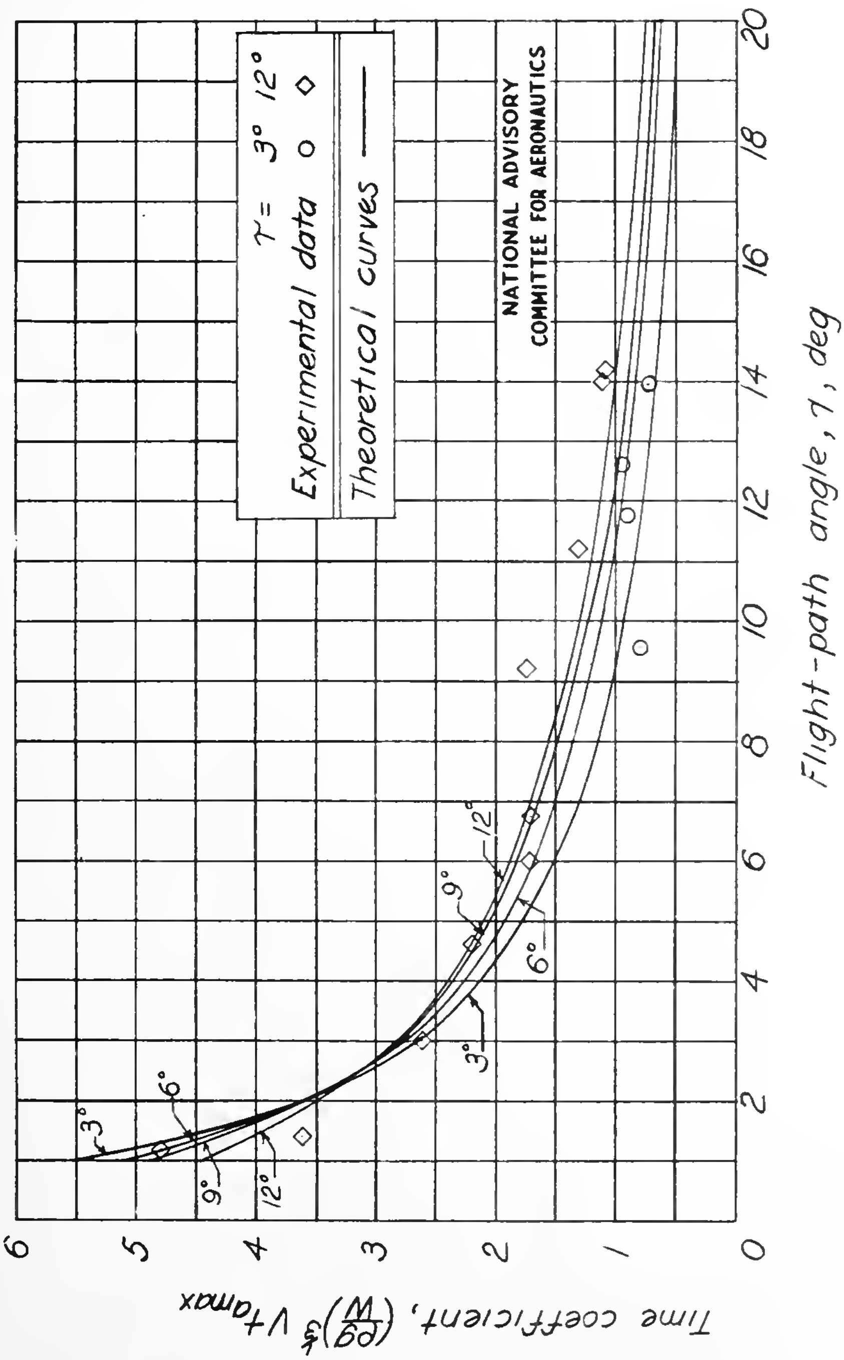

Figure 3.- Variation of time coefficient with flight-path angle for a prismatic float having an angle of dead rise of $22\frac{1}{2}°$.

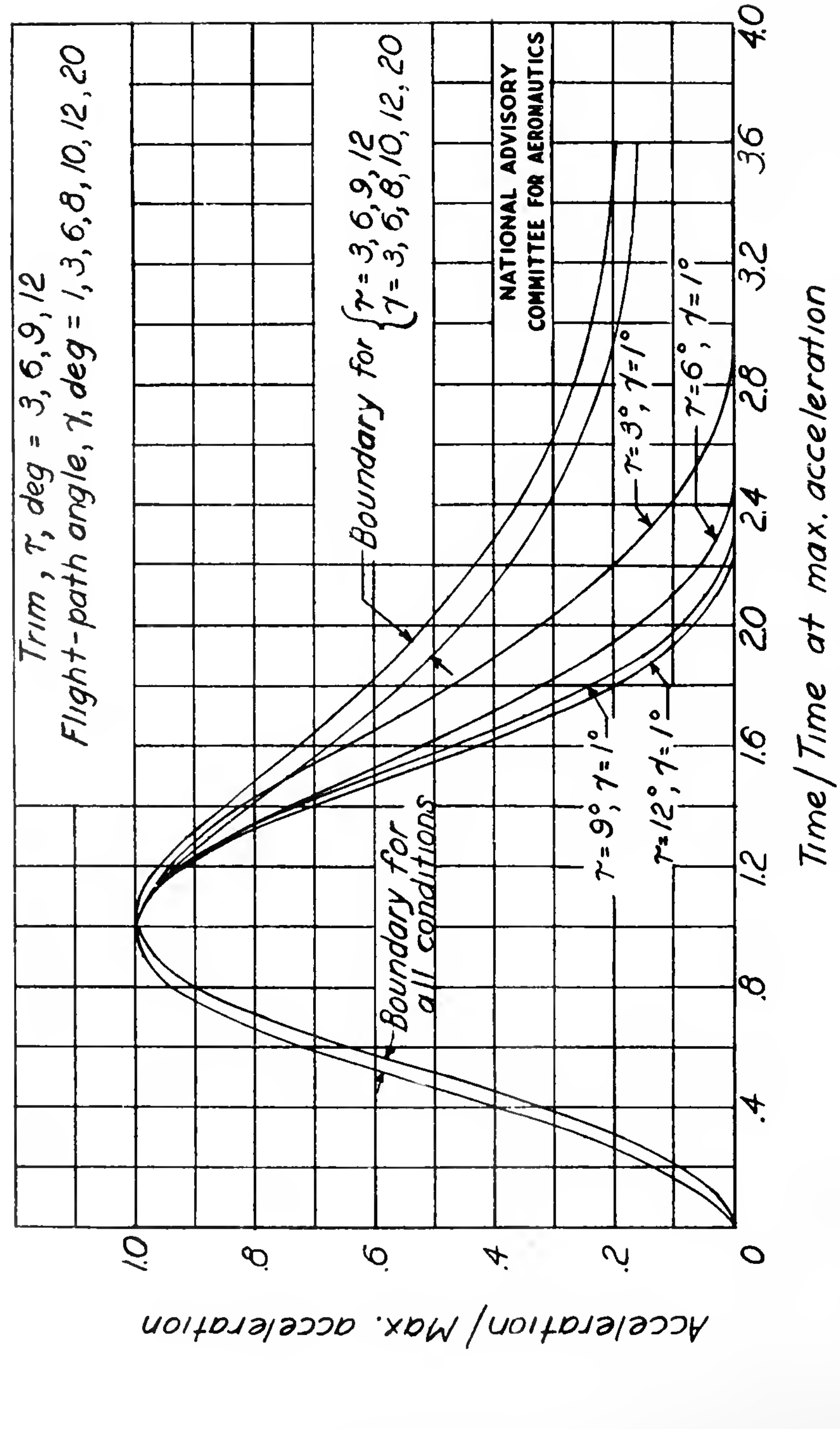

Figure 4.- Acceleration-time relation of impact for a prismatic float having an angle of dead rise of $22\frac{1}{2}^{\circ}$ (computed).